

$PD_{EVCS,k}$	Total EVCS charging demand, at hour k , p.u.
$PG_{i,k}, QG_{i,k}$	Active, reactive generation at hour k , p.u.
$PS_{i,k}, QS_{i,k}$	Active and reactive power injected through substation transformer at hour k , p.u.
R_k	Number of PEVs rejected from charging, at hour k
TN_k	Total number of PEVs charged simultaneously from all classes, at hour k
$TPch_k$	Total active power PEV charging demand from all class of vehicles, at hour k , p.u.
V_i	Bus voltage, p.u.
W_k	Number of PEVs waiting for service at hour k
δ	Voltage angle at a bus, rad.

II. INTRODUCTION

In Canada, the second highest source of greenhouse gas emissions is the transportation sector, and it is also one of the fastest growing contributors to the country's energy demand. According to Transport Canada, almost 35% of the total energy demand in Canada is from the transport sector [1]. The awareness that significant global warming is being caused by vehicular emissions is encouraging the transport sector to adopt plug-in electrical vehicles (PEV) [2].

However, increased number of PEVs can have a significant impact on power distribution system operational performance. Several studies show that the distribution grid can be significantly impacted by high penetration levels of PEVs [3-7]. The study of the impact of electric vehicle charging profiles dates back to the 1980s [3]. In [4], PEV charging control strategies are developed to mitigate distribution transformer ageing that could result from load peaks caused by PEV charging. The impact of uncoordinated PEV charging on system peak load, losses, voltage and system load factor are discussed in [5] and is noted to have adversely affected the efficiency of the distribution grid. It is shown in [6] that a 10% penetration of PEV may cause unacceptable variations in voltage profiles if there is no regulation on PEV charging, while coordinated charging can reduce system peak load, losses, and mitigate the impacts of uncoordinated PEV charging in the distribution system. The impact of PEV charging on a low voltage distribution network for various PEV penetrations is discussed in [7]; it is shown that PEV charging can have negative impacts in terms of increased peak load, increased power losses, overload of transformers and lines, voltage drop and increased voltage asymmetry.

Integration of DGs and PEVs have also been studied by researchers; in [8] an optimal power flow (OPF) based framework is used to examine the impact of PEV charging on distribution networks considering detailed models of wind and solar PV. Other researchers [9], [10] and [11] have also examined important aspects of the issue of coordination of DGs with PEVs.

Development of PEV charging load models has also been reported extensively in the literature. Monte Carlo simulation is used in [12] to generate virtual trip distances which consider driving habits, different vehicle models, etc., and hence formulate annual energy consumption model of light duty fleet

of PEVs. Queuing theory [13] based models have been proposed in [14]-[18] to model the PEV charging demand. The solution of a probabilistic constrained load flow problem with wind generation and PEV demand or supply is presented in [14] where the charging and discharging processes are represented using an M/M/ ∞ queuing model. A mathematical model that covers the spatial and temporal distribution of demand, based on fluid dynamic traffic model and queuing theory is developed in [15] to estimate the PEV charging demand for an electric vehicle charging station (EVCS). In [16], a max-weight PEV dispatch algorithm, based on a queuing formulation integrated with renewable energy sources is used to control the PEV charging in order to avoid costly distribution system infrastructure upgrades. In [17], a PEV demand model suitable for load flow studies is proposed wherein the charging demand is represented as a PQ bus with stochastic characteristics based on queuing theory. In [18], four different types of PEVs are considered and factors that affect their charging behavior, *e.g.*, differences in battery capacity and charging level, are discussed. A single PEV charging demand model is formulated and queuing theory is used to describe the behavior of multiple PEVs.

From the aforementioned literature review, it can be noted that the charging demand at an EVCS is affected by different factors, such as the number of PEVs arriving (λ), number of PEVs being charged simultaneously (N), the state of charge (SOC) of the battery, charging levels, battery capacity, charging duration, *etc.* Some of these parameters are independent processes, such as the arrival rate λ , and some are dependent on the PEV type such as battery capacity, or battery charging behavior (BCB), while some others are dependent on the PEV driving patterns, such as the SOC, the charging duration, *etc.* Note that, some of the parameters of the EVCS can be controlled effectively, such as N , the number of PEVs charging simultaneously. However, in order to do so, there is a need to effectively model the EVCS load as a function of various input parameters and controllable variables. So far, there is no reported work that examines how the EVCS load can be modeled as a smart load nor any attempt has been made to integrate the same within a larger operations framework of the distribution system.

Neural networks (NN) have been widely applied in various engineering applications such as system identification, signal enhancement, and noise cancellation. The power system literature has also seen many applications of NN; for example, in [19], the strategies to incorporate a NN-based load model into static and dynamic voltage stability are presented. In order to provide the forecasted load, NN is used in [20] to learn the relationship among past, current and future temperatures and loads. One standard application of NN is its use as a function approximation tool.

Moreover, different charging facilities have been studied by researchers for example; The day-time charging scenarios for PEVs at parking lots are studied in [21] using a two-stage approximate dynamic programming framework to determine the optimal charging strategies. A case study of a residential parking lot charging station [22] examines how many charging

spots can be reduced by encouraging customers to charge at off-peak hours, while in [23], an online management strategy is proposed that enables aggregators in public parking lots to dynamically manage PEV charging to maximize the owners' interest. However, these works consider Level-2 charging only, as against Level-3 charging in used in EVCS; and that charging at parking lots is carried out during office hours or late evening hours (residential lots) considering a specific class of customers; while an EVCS is more generic and need to use realistic arrival rates from mobility data, over a 24-hour period, for a wider range of customer class.

In the literature, two broad strategies for smart charging of PEVs are reported. In decentralized smart charging, the charging strategy is determined by individual PEV owners [24] while centralized smart charging strategy is generally determined by the Local Distribution Company (LDC) considering its own objectives and the charging schedule is communicated to the PEV owners [25]. In [26] a comparison between the centralized and decentralized charging strategies is made; and the advantages and disadvantages of each are presented. Other researchers [27], [28] and [29] have also examined important aspects such as real-time charging management for electric vehicles, demand response (DR) in smart distribution systems, and responsive end-user-based demand side management, respectively.

This paper presents a novel approach to model the EVCS load as smart load by proposing a Charging Station Controllable Load Estimator (CSCLE) which comprises a queuing model, used to construct the PEV charging data set as an input to a NN; and a NN model, to estimate the smart charging demand profile of the EVCS as a function of different parameters.

The $M_1/M_2/N$ queuing model considers the arrival rate of PEVs as a non-homogeneous Poisson process based on the travel patterns of light-duty vehicles in U.S., obtained from the 2009 National Household Travel Survey (NHTS) [30]. The queuing process integrates the SOC and BCB of the PEV battery within the service time. The output dataset of the queuing model is used to train the NN, to model the smart EVCS load.

The smart load model of the EVCS obtained from the CSCLE is then integrated within an optimal operations model of the distribution system that includes some new EVCS related control constraints. These comprehensive models of controlled

EVCS loads effectively introduce significant flexibility in distribution system operations and provide a DR service to the LDC. The main contributions of this paper are as follows:

- The CSCLE is developed using supervised NN learning to estimate the smart EVCS load as a function of the number of PEVs charging simultaneously, total charging current, PEV arrival rate at the EVCS, and time.
- The training set for the NN is constructed from a $M_1/M_2/N$ queuing model of the EVCS considering realistic arrival rates based on NHTS data, various class of PEVs, SOC and BCB of the PEV battery.
- The developed NN based smart load model of the EVCS is integrated within a novel distribution operations framework that considers PEV smart charging constraints, and EVCS related constraints. The smart operational decisions at the EVCS are determined from the perspectives of both the LDC and the EVCS owner.
- The EVCS smart charging framework can receive peak demand signals from the LDC and accordingly adjust its charging schedules to provide a DR service to the LDC. The contribution of such smart EVCS loads to DR and their integration in the distribution systems operation framework is examined.
- The smart EVCS operations are compared with an uncontrolled EVCS, to demonstrate the effectiveness and need for such a control scheme in smart grids.

The rest of this paper is organized as follows. The proposed novel framework and mathematical models for developing the EVCS smart load model and its integration in the distribution operations model are presented in Section III. In Section IV, the system description pertaining to the case study carried out, is presented. The results and discussions are presented in Section V and the concluding remarks in Section VI.

III. PROPOSED FRAMEWORK AND MATHEMATICAL MODELS

This paper proposes a smart distribution system operations framework including the DR contributions from a smart EVCS. The proposed framework is depicted in Fig.1, where the queuing model receives inputs from the NHTS dataset in terms of PEV class, battery capacity, SOC, etc., to construct the output profiles for the number of PEVs charged, total charging current, arrival rate, and time.

The queuing model considers the arrival of PEVs as a non-

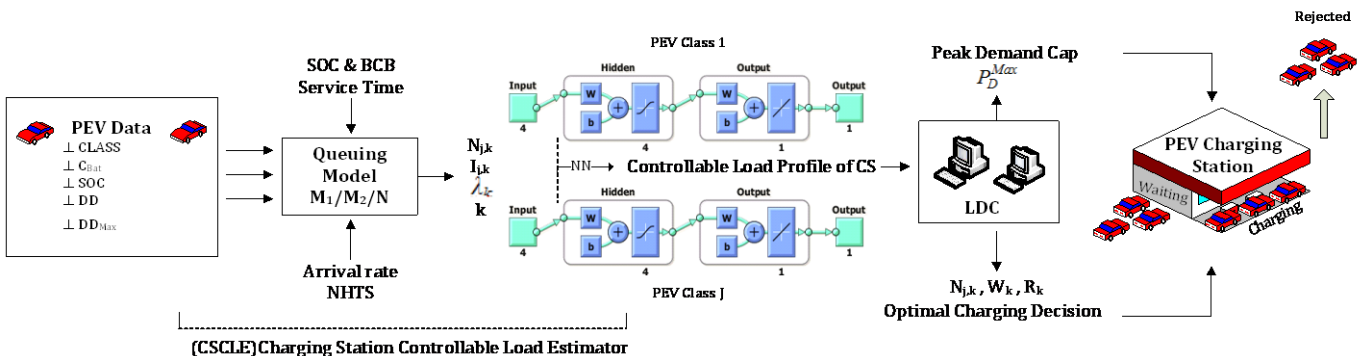


Fig.1: Interaction between LDC and EVCS.

homogeneous Poisson process and a novel piece-wise linear representation of the SOC is used to represent the BCB within the charging time in the $M_1/M_2/N$ queuing model.

The output profile from the queuing model serves as the training and validation data sets for the NN, to express the charging power for each class of PEV as a function of these parameters. The output of the CSCLE, developed using the supervised NN learning is integrated within the novel distribution operations model that considers PEV smart charging constraints, and EVCS related constraints to determine the smart operational decisions of the EVCS while considering various distribution operations constraints. As shown in Fig.1, the LDC sends a peak demand cap signal to the EVCS and which induces a DR services from the latter, whereby the PEVs are accordingly scheduled for charging.

A. Charging Station Controllable Load Estimator (CSCLE)

The EVCS smart load model is arrived at in two steps, as mentioned earlier. In the $M_1/M_2/N$ queuing model, M_1 denotes the arrival rate, modeled as non-homogeneous Poisson process based on NHTS dataset, M_2 denotes the service time of a PEV customer modeled using the SOC of the PEV considering the BCB, while N is the number of customers being served simultaneously. These data sets of PEV charging parameters obtained from the queuing model are then used in the second step, the NN model, as training and validation datasets to express the EVCS load as a function of different parameters.

The EVCS smart charging load profile considering all PEVs belonging to class j , is denoted by $Pch_{j,k}$ and can be expressed mathematically as a function of the number of PEVs being charged simultaneously ($N_{j,k}$), total charging current ($I_{j,k}$), arrival rate of PEVs at the EVCS (λ_k), and time (k), as follows:

$$Pch_{j,k} = f(N_{j,k}, I_{j,k}, \lambda_k, k). \quad (1)$$

As mentioned earlier, since k is an independent parameter, λ is independent process, and $I_{j,k}$ depends on the PEV class, the EVCS smart load in (1) can be represented as a function of $N_{j,k}$ only, as follows:

$$Pch_{j,k} = f(N_{j,k}). \quad (2)$$

From (2), it is evident that once the functional relationship between $N_{j,k}$ and $Pch_{j,k}$ is established using the NN, the EVCS smart load can be controlled by appropriate decisions on $N_{j,k}$.

The structure of the feed-forward NN used in this work is shown in Fig.2. The NN is trained in MATLAB using the Levenberg-Marquardt algorithm for back propagation. While training the NN, the entire dataset is divided into three subsets. The first subset is the training set, used for computing the gradient and updating the network weights and biases. The second subset is the validation set, which is used to monitor the error during the training process that normally decreases during the initial phase of training, as does the training set error. The third subset or test set is used to compare different models, using the test set error during the training process to evaluate the accuracy of the NN model. During the training process N_H

is varied to arrive at the best fit for the PEV charging load model.

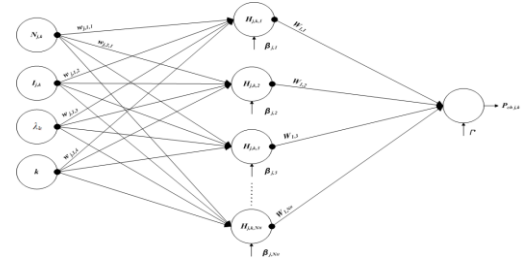


Fig.2: NN structure as part of CSCLE to determine smart EVCS load model.

In order to obtain a mathematical function of $Pch_{j,k}$ from the trained NN, the output from each hidden layer neuron $H_{j,k,1}$ to $H_{j,k,4}$ for different PEV classes are determined first. The incoming inputs with appropriate weights $w_{j,s,r}$ are summed up at each hidden layer neuron. Also, each hidden layer neuron has an additional input, the bias β_j to β_4 , which is used in the network to generalize the solution and to avoid a zero value of the output, even when an input is zero. This summed signal is passed through an activation function ($\tan sig$) associated with each hidden layer neuron, which transforms the net weighted sum of all incoming signals into an output signal from the hidden layer neuron. Accordingly,

$$H_{j,k,1} = \tan sig(w_{j,1,1}N_{j,k} + w_{j,1,2}I_{j,k} + w_{j,1,3}\lambda_k + w_{j,1,4}k + \beta_{j,1}) \quad (3)$$

$$H_{j,k,2} = \tan sig(w_{j,2,1}N_{j,k} + w_{j,2,2}I_{j,k} + w_{j,2,3}\lambda_k + w_{j,2,4}k + \beta_{j,2}) \quad (4)$$

$$H_{j,k,3} = \tan sig(w_{j,3,1}N_{j,k} + w_{j,3,2}I_{j,k} + w_{j,3,3}\lambda_k + w_{j,3,4}k + \beta_{j,3}) \quad (5)$$

$$H_{j,k,4} = \tan sig(w_{j,4,1}N_{j,k} + w_{j,4,2}I_{j,k} + w_{j,4,3}\lambda_k + w_{j,4,4}k + \beta_{j,4}) \quad (6)$$

In this work the NN is run for each PEV class individually. Finally, $Pch_{j,k}$ can be obtained from the output neuron of the trained NN as follows:

$$Pch_{j,k} = purelin(H_{j,k,1}W_{1,1} + H_{j,k,2}W_{1,2} + H_{j,k,3}W_{1,3} + H_{j,k,4}W_{1,4} + \Gamma) \quad (7)$$

where $purelin$ is a linear transfer function available in MATLAB.

B. Distribution Operations Model with Controllable EVCS

After all weights are determined, the distribution operations model is formulated by including the EVCS smart load model developed from the CSCLE framework, discussed in the previous subsection. Some new constraints are necessary to

capture the smart charging schedules and the smart EVCS operational aspects.

1) Objective Functions

Two different objective functions are considered, first is the minimization of feeder losses, which is the desired objective from the perspective of the LDC, and is given as follows:

$$J_1 = \frac{1}{2} \sum_{k=1}^{24} \left[\sum_{i=1}^{N_B} \sum_{j=1}^{N_B} G_{i,j} \left(V_{i,k}^2 + V_{j,k}^2 - 2V_{i,k}V_{j,k} \cos(\delta_{j,k} - \delta_{i,k}) \right) \right]. \quad (8)$$

The second is the maximization of the number of PEVs services or charged at the EVCS over a day, representing the perspective of the EVCS owner, and is given as follows:

$$J_2 = \sum_{k=1}^{24} \sum_{j=1}^J N_{j,k}. \quad (9)$$

2) Demand Supply Balance

The demand supply balance for active and reactive power is given by the power flow equations, augmented by including the total EVCS smart load at the EVCS bus to the active power equation, as follows:

$$PG_{i,k} - PD_{i,k} = \sum_{j=1}^{N_B} f(V_{i,k}, \delta_{i,k}) \quad \forall i, i \neq cs \quad (10)$$

$$PG_{cs,k} - PD_{cs,k} - TPch_{cs,k}(N_k) = \sum_{j=1}^{N_B} f(V_{cs,k}, \delta_{cs,k}) \quad (11)$$

$$QG_{i,k} - QD_{i,k} = - \sum_{j=1}^{N_B} f(V_{i,k}, \delta_{i,k}) \quad \forall i \quad (12)$$

Where

$$TPch_{cs,k}(N_k) = \sum_{j=1}^J Pch_{j,k}(N_{j,k}). \quad (13)$$

In (13) the total charging power $TPch_{cs,k}$ at the EVCS at hour k is the sum of the charging powers of each class of PEVs and is included in (11) at the specific bus where the EVCS is located. It is to be noted that $TPch_{cs,k}$ is a decision variable, unlike most other works, and is optimally determined from the model solution, by optimally determining N_k . It is to be noted that the PEV charging load has been modeled in this work as real power demand only. The PEV battery systems are typically considered to be unity power factor loads as per the common practice [16], [17], [18]. In some recent works, researchers have examined how PEVs can provide reactive power support services to the grid through capacitor banks associated with PEV batteries and chargers [31], [32], which is however not considered in this paper, in order to focus on the stated objectives.

3) Controlled Operation of EVCS

These constraints pertain to EVCS smart operation by effective control of the number of PEVs charging simultaneously, N_k , number of PEVs waiting for charging, W_k , and the number of PEVs rejected for charging, R_k . Accordingly,

the total number of PEVs charging simultaneously at hour k , is given by:

$$TN_k = \lambda_k - W_k - R_k \quad (14)$$

where TN_k is the sum of the number of PEVs, across all classes, charging simultaneously at hour k , and is given by:

$$TN_k = \sum_{j=1}^J N_{j,k}. \quad (15)$$

Also, in (14), R_k is given by:

$$R_k = \lambda_k - (TN_k + W^{Max}). \quad (16)$$

The total number of PEVs being charged simultaneously at hour k , is constrained by the EVCS capacity, as follows:

$$TN_k \leq N^{Max}. \quad (17)$$

Furthermore, the EVCS may also impose limits on the maximum number of PEVs of a particular class that can be charged at a time. Hence, the following constraint is imposed:

$$N_{j,k} \leq N_j^{Max}. \quad (18)$$

The maximum number of PEVs that can wait for charging at hour k , are constrained by the EVCS space availability and is given by:

$$W_k \leq W^{Max}. \quad (19)$$

4) Limit on EVCS Peak Demand

In order to ensure that the EVCS charging demand does not create additional peaks in the LDC's load profile, the following constraint is added:

$$\underline{TPD} \leq PD_{EVCS,k} \leq \overline{TPD} \quad (20)$$

Where $PD_{EVCS,k}$ denotes the total charging demand of the EVCS at hour k , \underline{TPD} represents the minimum charging load as defined in the agreement with the EVCS owner, as a DR provider, while, \overline{TPD} specifies the maximum peak demand of the EVCS allowed by the LDC.

In addition to the above, the system operational constraints such as bus voltage limits and substation capacity limits are also imposed. The above NLP model is solved using the MINOS5.1 solver in GAMS environment.

IV. CASE STUDY SYSTEM

A. Distribution System Topology

The analysis presented in this paper is carried out considering the IEEE 69-bus radial distribution system, whose single line-diagram is given in Fig.3 [33]. The distribution system is supplied through the substation at bus-1. It is assumed that an EVCS is arbitrarily located at bus-59, without any loss of generality.

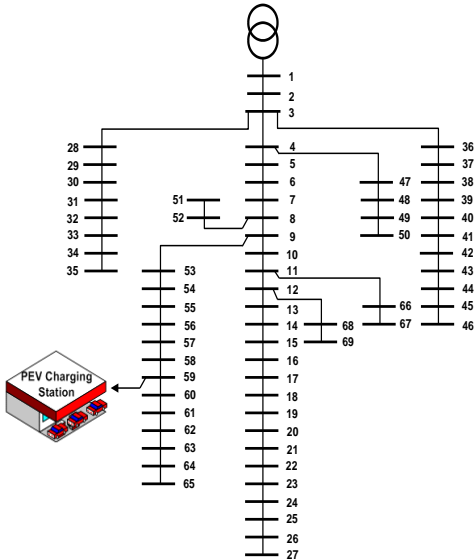


Fig.3: 69-Bus radial distribution system [33].

B. NHTS Data and Modeling PEV Arrival Rate

Since the availability of data pertaining to penetration of PEVs and PEV charging load recordings are still very limited, NHTS 2009 [30] data for light-duty vehicles is used in this work to model the PEV charging demand. The dataset comprises information on 12,469 vehicles, of four specific class of vehicles- automobile car, sports utility vehicle (SUV), van, and pickup truck; with the arrival destination being to buy gas at the gas-station, assuming that PEVs have the same pattern for arriving at the EVCS for charging their vehicles.

With this large dataset of information, the arrival rate of PEVs is realistically modelled for a large range of customer classes; the normalized hourly distribution of PEVs arriving for charging is presented in Fig.4. Furthermore, in order to draw the correspondence between fuel-driven vehicles and PEVs for the data processing work, in this paper, four different PEV classes have been used with their appropriate battery sizes to match the NHTS classes, as given in Table I. Nevertheless, the developed modeling framework is generic and demonstrates its effectiveness, and any appropriate realistic arrival rate data from an EVCS may be used to determine actual schedules and rejections.

TABLE I
PEV PARAMETERS FOR CHARGING LOAD MODEL

NHTS Class [30]	Automobile Car	SUV	Van	Pickup Truck
PEV Class	Compact	Economy	Mid-size Van	Light Truck
B^{Cap} , kWh	8 - 12	10 - 14	14 - 18	19 - 23
E_C , kWh/mile	0.2- 0.3	0.25-0.35	0.35-0.45	0.48-0.58
DD, miles	Lognormal Distribution, $\mu_M = 40$ miles, $\sigma_M = 20$ miles			

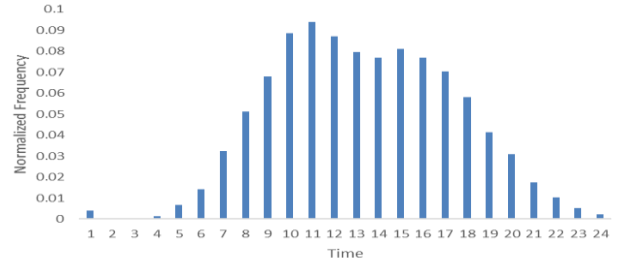


Fig.4: Arrival rate frequency distribution.

C. Neural Network

In this work, the vehicular data for 90 days is used considering 24, one-hour time intervals per day. There are four input layer neurons corresponding to the four inputs- N , I , λ , and k , and one output layer neuron corresponding to the output Pch . The NN has one hidden layer with $N_H = 4$, i.e., four hidden layer neurons; this was obtained by various trial simulations. An input matrix of dimension 4×2160 is created from the queuing model simulations, while the output vector is of dimension 1×2160 . For this study, the data division ratios between the training, validation, and test sets are assumed to be 0.7, 0.15, and 0.15, respectively.

V. RESULTS AND DISCUSSIONS

The NN is used to model the controllable EVCS load in terms of controllable variables and parameters from the perspective of the LDC and the EVCS owner. Four MATLAB functions for data division are used to train the NN, as discussed earlier, in order to identify the best function to divide the data sets into training, validation and testing subsets, and the corresponding values of R-squared are compared. The estimated total EVCS load, using the proposed NN, is compared with that from a PEV charging data set obtained from the queuing model and is observed to be very closely matching. It is also noted that the function *dividerand* best captures the EVCS charging demand estimate (Fig.5).

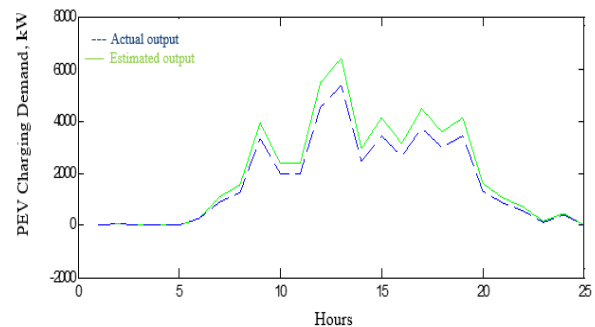


Fig.5: Estimated output using the *dividerand* function of the NN toolbox.

A. Controlled Operation of EVCS: LDC Perspective

This case assumes that the distribution system is operated from the LDC's perspective, and the EVCS smart operation is accordingly determined. The typical criterion for LDCs operation, as mentioned earlier, is minimization of losses, given by (8). Fig.6 presents the optimal number of PEVs to be charged, which remains the same with or without consideration

of the class capacity constraint (18). It is to be noted that although the number of PEVs to be served are optimally distributed over the day, a significant number are rejected during hours 9-17 when the arrival rate is high, even though the EVCS capacity is not reached. This is because of the choice of the objective function, *i.e.*, the loss minimization perspective of the LDC. Further, when the class capacity constraint (18) is considered, although the total number of PEVs being charged does not change, it does bring about some changes in the number of PEVs of a given class being charged at an hour, as seen from Fig.7 and Fig.8.

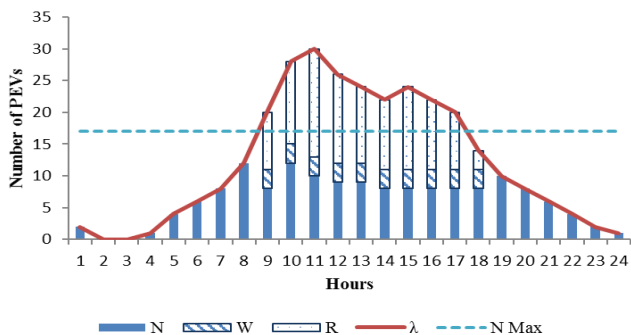


Fig.6: Optimal PEV schedule at EVCS, LDC Perspective.

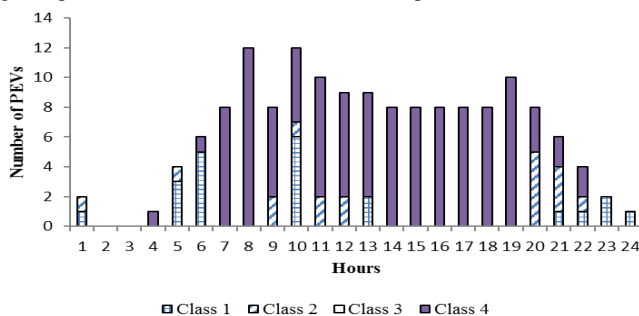


Fig.7: Optimal number of PEVs served without considering class constraints, LDC Perspective.

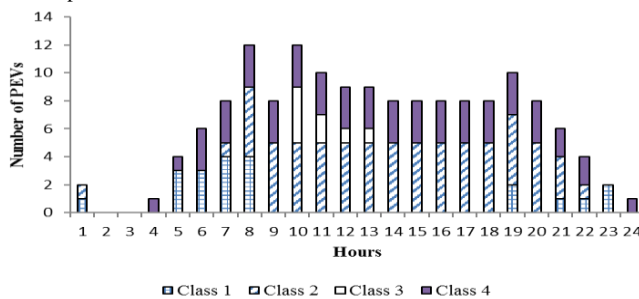


Fig.8: Optimal number of PEVs served considering class constraints, LDC Perspective.

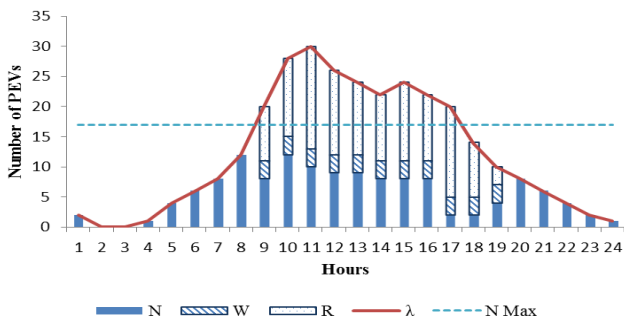


Fig.9: Optimal PEV schedule at EVCS considering P_{Max} , LDC Perspective.

Figs.9-12 present the optimal number of PEVs to be charged, overall system demand, voltage profile at Bus-59, and PEV charging demand at Bus-59 respectively, considering limits on the EVCS peak demand (20). This represents a situation in smart grid environment, where the LDC sends a peak demand signal to the EVCS on an hour-to-hour basis, and the EVCS incorporates this control signal as an additional constraint in its charging schedule. Essentially the EVCS therefore provides a DR service to the LDC. Figs.9-12 demonstrate that the LDC can indeed improve system operation, reduce the peak load, and alleviate the need for network augmentation in the presence of PEV charging loads.

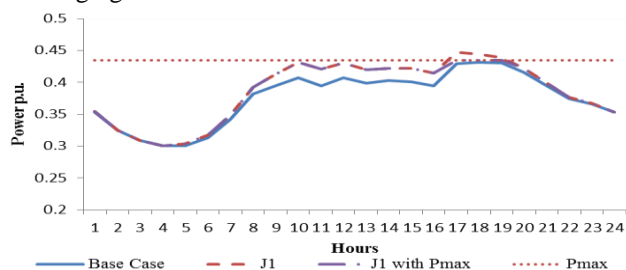


Fig.10: System demand without, with optimal EVCS demand, LDC Perspective.

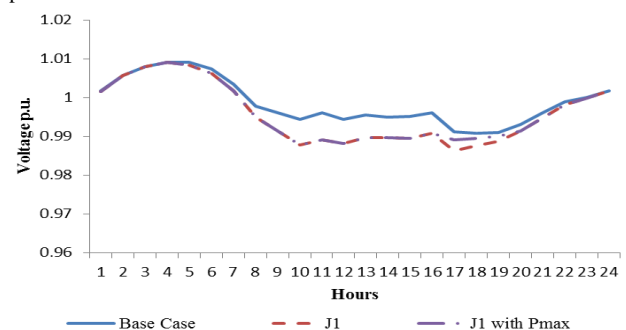


Fig.11: Voltage profile at Bus-59 for controlled EVCS, LDC Perspective.

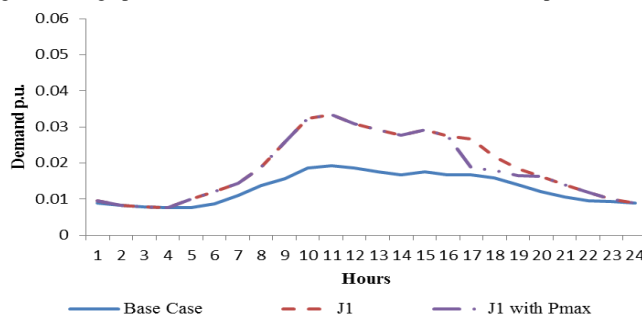


Fig.12: Total PEV charging demand at Bus-59, LDC Perspective.

B. Controlled Operation of EVCS: Owner's Perspective

This case assumes that the LDC operates the distribution system taking into account the interests of the EVCS owner, while adhering to system operational constraints. To this effect the objective is to maximize the number of PEVs being charged simultaneously, given by (9). Fig.13, presents the optimal number of PEVs to be charged, with and without the class capacity constraint (18). It is noted that N is optimally distributed over the day, and the number of PEVs to be served is significantly higher as compared to when the LDC operated to minimize system losses.

It is noted that the EVCS operates at full capacity, *i.e.*, $N = N^{Max}$, during hours 9-17 when the arrival rate is high (Fig.13) and the number of vehicles refused charging, is much less. The total number of PEVs being served at an hour, with or without the class constraint (18) is found to be the same, although the class-wise distribution of charging does vary when (18) is included, as seen from Fig.14 and 15.

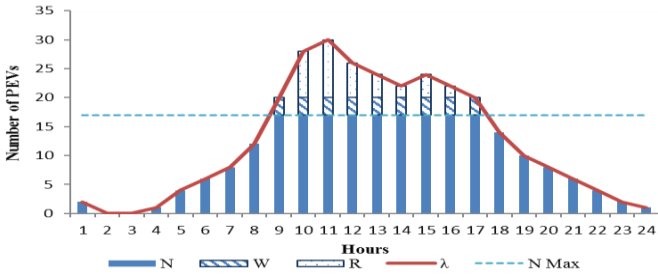


Fig.13: Optimal PEV schedule at EVCS, Owner's Perspective.

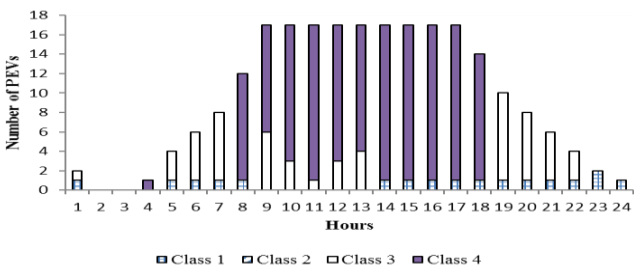


Fig.14: Optimal number of PEVs served without class constraints, Owner's Perspective.

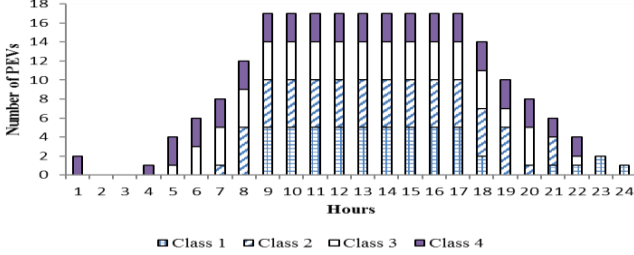


Fig.15: Optimal number of PEVs served considering class constraints, Owner's Perspective.

Figs.16-19 present the optimal number of PEVs to be charged, overall system demand, voltage profile at Bus-59, and PEV charging demand at Bus-59, respectively, considering the peak demand limit (20). Figs.16 demonstrates that the optimal number of PEVs charged is much lower when (20) is included, as compared to the case without (20), which results in less power drawn by the LDC from the external grid (Fig.17), and much improved voltage profiles (Fig.18), and the EVCS provides a DR service by reducing its charging demand as seen in Fig.19.

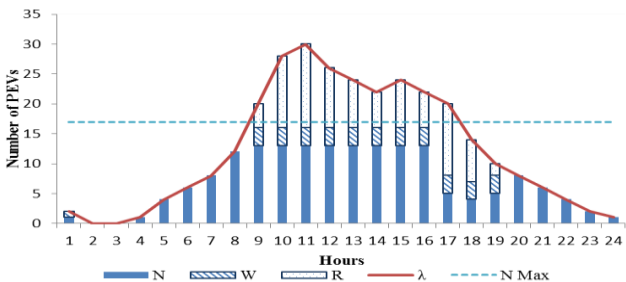


Fig.16: Optimal PEV schedule at EVCS, Owner's Perspective.

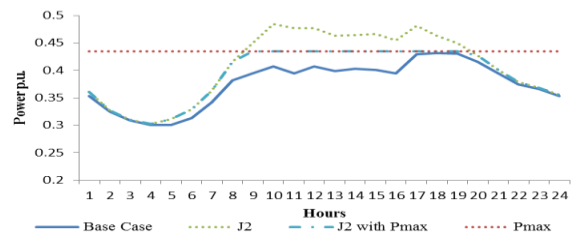


Fig.17: System demand without, with optimal EVCS demand: Owner's Perspective.

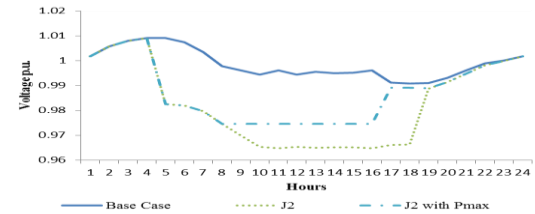


Fig.18: Voltage profile at Bus-59 for controlled EVCS, Owner's Perspective.

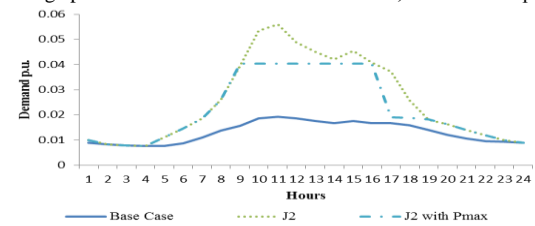


Fig.19: Total PEV charging demand at Bus-59, Owner's Perspective.

A comparison of uncontrolled EVCS versus controlled EVCS with different objective functions, without and with (20), is presented in Table II. The revenue earnings for the EVCS (REV) are calculated considering winter Time-of-Use prices applicable in Ontario, Canada [34]. It is noted that uncontrolled operation of the EVCS accommodates more PEVs for charging and hence yields a high revenue (136.7 \$/day) for the EVCS, but consequently requires much more power drawal from the external grid (13.11 p.u.), and results in high system losses (0.93 p.u.).

Controlled operation of the EVCS from the owner's perspective, *i.e.*, with the objective of maximizing N , results in a reduction in total number of PEVs charged/day (TN) to 231 PEVs, as compared to uncontrolled EVCS operation where 294 PEVs are charged. An increased number of vehicles are kept on waiting or are rejected. The EVCS revenue reduces to 99.6 \$/day. When the peak demand constraint (20) is imposed, TN further reduces to 171 PEVs, the revenue of EVCS dips to 95.5 \$/day.

Finally, the controlled operation of the EVCS from the LDC's perspective, *i.e.*, with the objective of minimizing losses, results in a further reduction in TN to 152 PEVs without (20) and 134 PEVs when (20) is imposed. The EVCS revenue reduces to 93.4 \$/day.

It is therefore noted that the EVCS provides a DR service to the LDC after a peak demand signal is received, and the EVCS incorporates this as an additional constraint (20) in its charging schedule. It is noted that the LDC can indeed improve system operation, reduce the peak load, and alleviate the need for network augmentation in the presence of PEV charging loads compared without peak demand constraint scenario for both perspectives (Table II).

TABLE II
COMPARISON OF ALL CASES AND SUMMARY BENEFITS

	Controlled EVCS				Uncontrolled
	Objective: Min {Loss}		Objective: Max {N}		
	No P_{Max} constraint	With P_{Max} constraint	No P_{Max} constraint	With P_{Max} constraint	
TN	152	134	231	171	294
REV	93.8	93.4	99.6	95.5	136.7
TL	0.335	0.328	0.471	0.391	0.93
TP	9.27	9.24	9.78	9.44	13.11

TN: Total number of PEVs charged/day
 REV: EVCS revenue, \$/day
 TL: Total system loss, p.u./day
 TP: Total energy drawn from grid by EVCS, p.u./day

It is noted that controlled operation of the EVCS has some impact on the distribution system performance. Fig.20 shows that as expected, the total EVCS load is significantly increased when the EVCS owner’s perspective (*maximizing J_2*) is considered as compared to the LDC’s perspective (*minimizing J_1*). The bus voltage profiles are also affected by PEV charging (Fig.21). For example, at Bus-59, which is the EVCS bus, significant voltage drop takes place at various hours, depending on the operations perspective. In case of the EVCS owner’s perspective the voltage profiles are significantly deteriorated, although they are within the operating limits of 0.95 p.u., while in the LDC’s perspective the voltage profile is significantly better. A comparison of the controlled EVCS operation from both perspectives, at Bus-59, are presented in Fig.22; the increase in the demand due to EVCS charging is significant considering the owner’s perspective as compared to the LDC’s perspective.

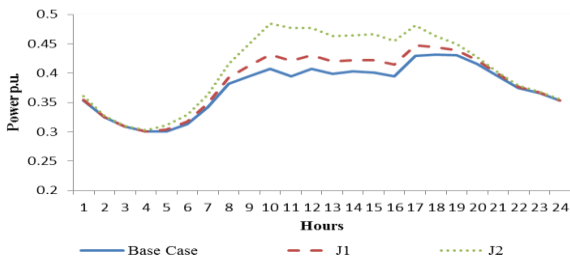


Fig.20: Comparison of system demand without and with optimal EVCS demand.

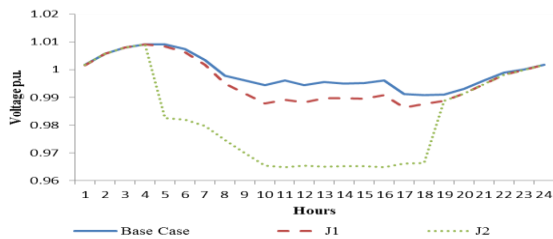


Fig.21: Comparison of voltage profile at Bus-59 for controlled EVCS demand.

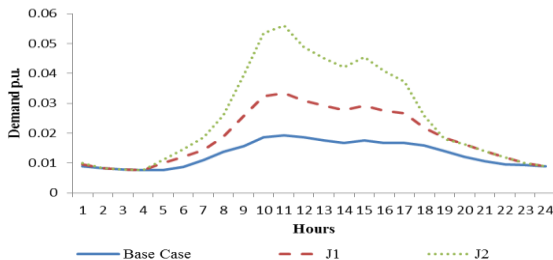


Fig.22: Total PEV charging demand at Bus-59 for both perspectives.

C. Uncontrolled Operation of Charging Station

This subsection captures the impact of controlled EVCS load (modeled as per the proposed approach) and compares that with uncontrolled EVCS operation, using the EVCS load estimated using the queuing model. Uncontrolled operation of the EVCS means, all PEVs arriving for charging, at any time, irrespective of the arrival rate, are right away provided a charging service. The expected uncontrolled EVCS load (Fig.23) is significantly increased depending on the arrival rate of PEVs, as compared to the case with no PEV.

The expected voltage profile at Bus-65 for uncontrolled operation of EVCS is given in Fig.24. As expected, the voltage profile drops significantly coinciding with the appearance of EVCS loads during hours 9–17. While, as noted earlier in the LDC controlled operation of EVCS, from either LDC’s or EVCS owner’s perspectives, the voltage profiles are significantly better (Fig.21). This demonstrates that the LDC can easily and smartly accommodate significant amount of PEV charging loads considering appropriate control strategies for the EVCS.

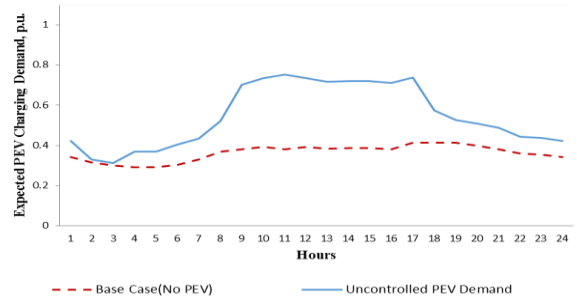


Fig.23: Expected uncontrolled charging demand.

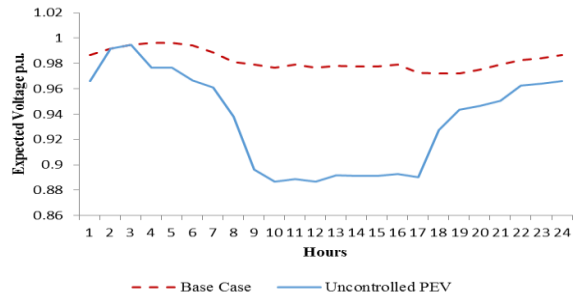


Fig.24: Expected voltage profile at Bus-65 for uncontrolled PEV charging.

VI. CONCLUSIONS

This paper presented the comprehensive modeling of EVCS load using controllable variables such as- the number of PEVs being charged simultaneously, total charging current, arrival rate, and time. The work further examined the contribution of such smart EVCS loads to DR and their integration in the distribution systems operations framework. The controllable load profile of EVCS was obtained using the novel framework for CSCLE. The CSCLE comprised a queuing model that considered several classes of vehicles, arriving at the EVCS as a non-homogeneous Poisson process, and determined the charging load for each. This dataset was used to train a NN and hence to determine the controllable charging load model of the EVCS.

The charging load model was integrated with a distribution optimal operations model to obtain the optimal charging decisions for the EVCS. Two different objective functions were considered, minimizing total feeder losses which represented the LDC's perspective; and maximizing the number of PEVs charged simultaneously, representing the EVCS owner's perspective. A 69-bus distribution system test case was presented to study the controlled operation of EVCS loading and its contribution to DR service.

It was noted from the studies that the EVCS owner's objective of maximizing the number of PEVs being charged simultaneously, can result in deterioration of bus voltages, and high feeder losses while accommodating more PEVs for charging, and rejecting only a few. On the other hand, the LDC's perspective of minimizing feeder losses resulted in significant rejections and wait times.

REFERENCES

- [1] Transport Canada [Online]. Available: <http://www.tc.gc.ca/environment/menu.htm#climatechange>
- [2] M. Duvall and E. Knipping, "Environmental assessment of plug-in hybrid electric vehicles," Electric Power Research Institute (EPRI), 2007.
- [3] G. T. Heydt, "The impact of electric vehicle deployment on load management strategies," *IEEE Transactions on Power Apparatus and Systems*, vol. 1, no. 144, pp. 1253–1259, May 1983.
- [4] Q. Gong, S. Midlam-Mohler, E. Serra, V. Marano, and G. Rizzoni, "PEV charging control considering transformer life and experimental validation of a 25 kVA distribution transformer," *IEEE Transactions on Smart Grid*, vol. 6, no. 2, Mar 2015.
- [5] K. Clement-Nyns, E. Haesen, and J. Driesen, "The impact of charging plug-in hybrid electric vehicles on a residential distribution grid," *IEEE Transactions on Power Systems*, vol. 25, no.1, pp. 371–380, Feb 2010.
- [6] E. Sortomme, M. M. Hindi, S. D. MacPherson, and S. S. Venkata, "Coordinated charging of plug-in hybrid electric vehicles to minimize distribution system losses," *IEEE Transactions on Smart Grid*, vol. 2, no. 1, Mar 2011.
- [7] A. Bosovic, M. Music, S. Sadovic, "Analysis of the impacts of plug-in electric vehicle charging on the part of a real low voltage distribution network", PowerTech, Eindhoven, 2015.
- [8] O. Hafez and K. Bhattacharya, "Optimal PHEV charging in coordination with distributed generation operation in distribution systems", Proc. IEEE PES General Meeting 2012, San Diego, USA.
- [9] W. Tushar, C. Yuen, S. Huang, D. B. Smith, and H. V. Poor, "Cost minimization of charging stations with photovoltaics: an approach with EV classification", *IEEE Transaction on Intelligent Transportation System*, vol. 17, no. 1, pp. 156-169, January 2016.
- [10] M. Takagi, "Economic value of PV energy storage using batteries of battery-switch stations", *IEEE Trans. Sustain. Energy*, vol. 4, no. 1, pp. 164–173, Jan. 2013.
- [11] M. Brenna, A. Dolara, F. Foiadelli, S. Leva, and M. Longo, "Urban scale photovoltaic charging stations for electric vehicles", *IEEE Trans. Sustain. Energy*, vol. 5, no. 4, pp. 1234–1241, Oct. 2014.
- [12] M. F. Shaaban, Y. M. Atwa, and E. F. El-Saadany, "PEVs modeling and impacts mitigation in distribution networks," *IEEE Transactions on Power Systems*, vol. 28, no. 2, May 2013.
- [13] Adan, I., and Resing, J., "Queueing theory", available at: <http://www.win.tue.nl/~iadan/queueing.pdf>, Department of Mathematics and Computing Science, Eindhoven University of Technology, The Netherlands, 2002.
- [14] J. G. Vlachogiannis, "Probabilistic constrained load flow considering integration of wind power generation and electric vehicles," *IEEE Transactions on Power Systems*, vol. 24, no. 4, pp. 1808–1817, Nov 2009.
- [15] S. Bae, and A. Kwasinski, "Spatial and temporal model of electric vehicle charging demand," *IEEE Transactions on Smart Grid*, vol. 3, no. 1, Mar 2012.
- [16] Q. Li, R. Negi, and M. D. Ilić, "A queueing based scheduling approach to plug-in electric vehicle dispatch in distribution systems", [Online]. Available: <http://arxiv.org/pdf/1203.5449v1.pdf>.
- [17] R. Garcia-Valle and J. G. Vlachogiannis, "Electric vehicle demand model for load flow studies," *IEEE Transactions on Electric Power Components and Systems*, vol. 37, no. 5, pp. 577–582, May 2009.
- [18] G. Li and X. Zhang, "Modeling of plug-in hybrid electric vehicle charging demand in probabilistic power flow calculations," *IEEE Transactions on Smart Grid*, vol. 3, no. 1, Mar 2012.
- [19] D. Chen and R. Mohler, "Neural-network-based load modeling and its use in voltage stability analysis," *IEEE Transactions on Control Systems Technology*, vol. 11, no. 4, pp. 460–470, July 2003.
- [20] D. Park, M. El-Sharkawi, I. Marks, R.J., L. Atlas, and M. Damborg, "Electric load forecasting using an artificial neural network," *IEEE Transactions on Power Systems*, vol. 6, no. 2, pp. 442–449, May 1991.
- [21] A. L. Zhang, and Y. Li, "Optimal management for parking-lot electric vehicle charging by two-stage approximate dynamic programming", *IEEE Transactions on Smart Grid (in print)*.
- [22] B. H. Zhang, Z. Hu, Z. Xu, and Y. Song, "Optimal planning of PEV charging station with single output multiple cables charging spots" *IEEE Transactions on Smart Grid, (in print)*.
- [23] C. E. Akhavan-Rezai, M. Shaaban, E. El-Saadany, and F. Karray, "Online intelligent demand management of plug-in electric vehicles in future smart parking lots", *IEEE Systems Journal (in print)*.
- [24] C. K. Wen, J. C. Chen, J. H. Teng, and P. Ting, "Decentralized plug-in electric vehicle charging selection algorithm in power systems," *IEEE Transaction on Smart Grid*, vol. 3, no. 4, pp. 1779 -1789, Dec. 2012.
- [25] H. Liu, Z. Hu, Y. Song, J. Wang, and X. Xie, "Vehicle-to-grid control for supplementary frequency regulation considering charging demands," *IEEE Transaction on Power System*, vol. 30, no. 6, pp. 3110-3119, November 2015.
- [26] P. Richardson, D. Flynn, and A. Keane, "Local versus centralized charging strategies for electric vehicles in low voltage distribution systems," *IEEE Transaction on Smart Grid*, vol. 3, no. 2, pp. 1020-1028, June 2012.
- [27] S. I. Vagropoulos, D. K. Kyriazidis and A. G. Bakirtzis, "Real-time charging management framework for electric vehicle aggregators in a market environment," *IEEE Transactions on Smart Grid*, vol. 7, no. 2, pp. 948-957, March 2016.
- [28] H. S. V. S. Kumar Nunna and S. Doolla, "Demand response in smart distribution system with multiple microgrids," *IEEE Transactions on Smart Grid*, vol. 3, no. 4, pp. 1641-1649, Dec. 2012.
- [29] H. S. V. S. Kumar Nunna and S. Doolla, "Responsive end-user-based demand side management in multimicrogrid environment," *IEEE Transactions on Industrial Informatics*, vol. 10, no. 2, pp. 1262-1272, May 2014.
- [30] Summary of travel trends: 2009 National Household Travel Survey, Federal Highway Administration, USA, 2012 [Online]. Available: <http://nhts.ornl.gov/2009/pub/stt.pdf>.
- [31] G. M. Kisacikoglu, B. Ozpineci, and L. Tolbert, "EV/PHEV bidirectional charger assessment for V2G reactive power operation," *IEEE Trans. Power Electron.*, vol. 28, no. 12, pp. 5717-5727, 2013.
- [32] H. M. Falahi, H. Chou, M. Ehsani, L. Xie, and K. Purry, "Potential power quality benefits of electric vehicles," *IEEE Trans. Sustainable Energy*, vol. 4, no. 4, pp. 1016-1023, 2013.
- [33] M. E. Baran and F. F. Wu, "Optimal sizing of capacitor placed on radial distribution systems," *IEEE Trans. Power Del.*, vol. 4, no. 1, pp. 735–743, Jan. 1989.
- [34] Ontario hydro Time of use pricing rates [Online]. Available: http://www.ontario-hydro.com/index.php?page=current_rates.



Omar Hafez (S'11) received the BSc degree from Umm Al-Qura University, Makkah, Saudi Arabia, in 2004 in Electrical and Computer Engineering, and the MASc degree in Electrical and Computer Engineering from the University of Waterloo, Waterloo, ON, Canada, in 2011, where he is currently pursuing the Ph.D. degree. His research interests include micro-grids, renewable DG, distribution system operation and planning, electric vehicles, and smart grids.



Kankar Bhattacharya (M'95–SM'01) received the Ph.D. degree in Electrical Engineering from the Indian Institute of Technology, New Delhi, in 1993. He was in the faculty of Indira Gandhi Institute of Development Research, Mumbai, India (1993–1998) and then the Department of Electric Power Engineering, Chalmers University of Technology Göteborg, Sweden (1998–2002). He has been with the Department of Electrical and Computer Engineering, University of Waterloo, Waterloo, ON, Canada, since 2003 and is currently a full Professor. His research interests are in power system economics and operational aspects.